Molecular Nutrition & Food Research

www.mnf-journal.com

Transcriptional Response of White Adipose Tissue to Withdrawal of Vitamin B3

*Wenbiao Shi, Maria A. Hegeman, Atanaska Doncheva, Inge van der Stelt, Melissa Bekkenkamp-Grovenstein, Evert M. van Schothorst, Charles Brenner, Vincent C. J. de Boer, and Jaap Keijer**

Scope: Distinct markers for mild vitamin B3 deficiency are lacking. To identify these, the molecular responses of white adipose tissue (WAT) to vitamin B3 withdrawal are examined.

Methods and results: A dietary intervention is performed in male C57BL/6JRccHsd mice, in which a diet without nicotinamide riboside (NR) is compared to a diet with NR at the recommended vitamin B3 level. Both diets contain low but adequate level of tryptophan. Metabolic flexibility and systemic glucose tolerance are analyzed and global transcriptomics, qRT-PCR, and histology of epididymal WAT (eWAT) are performed. A decreased insulin sensitivity and a shift from carbohydrate to fatty acid oxidation in response to vitamin B3 withdrawal are observed. This is consistent with molecular changes in eWAT, including an activated MEK/ERK signaling, a lowering of glucose utilization markers, and an increase in makers of fatty acid catabolism, possibly related to the consistent lower expression of mitochondrial electron transport complexes. The synthesis pathway of tetrahydropteridine (BH4), an essential cofactor for neurotransmitter synthesis, is transcriptionally activated. Genes marking these processes are technically validated.

Conclusion: The downregulation of *Anp32a*, *Tnk2* and the upregulation of *Mapk1*, *Map2k1*, *Qdpr*, *Mthfs*, and *Mthfsl* are proposed as a WAT transcriptional signature marker for mild vitamin B3 deficiency.

1. Introduction

Vitamin B3 represents nicotinic acid, nicotinamide, nicotinamide mononucleotide, and nicotinamide riboside (NR), which are precursors of nicotinamide adenine dinucleotide (NAD^+).[1] NAD^+ supports multiple essential cellular functions and is principally involved in redox reactions, as electron acceptor (NAD^+) or donor (NADH).[2]

In mammals, NAD^+ can also be synthesized from the essential amino acid tryptophan (Trp).[3] Long-term inadequate intake of vitamin B3 and Trp can lead to the development of Pellagra in humans. Pellagra has a number of unspecific symptoms, including lesions of the skin, soreness of tongue and mouth, diarrhoea, and dementia. Weakness and fatigue are early symptoms of this disease. Pellagra can ultimately result in death due to multi-organ failure, when not treated.[4] Rats fed a vitamin B3-free and Trp-limited diet can show a pellagra-like phenotype.[5,6]

In terms of contribution to NAD^+ level, dietary Trp is equivalent to vitamin B3 in a ratio of approximately 1/60 in humans,[7] while this ratio is slightly higher in mice.[8] The conversion of Trp to NAD^+ is dependent on Trp intake, since lower Trp intake prioritizes tryptophan for protein synthesis.[9] Trp is also required for the biosynthesis of the neurotransmitter serotonin. In mice, 0.1% tryptophan in the diet is considered to be an adequate level of intake for normal growth.[10,11] A higher intake of Trp may negate the consequences of vitamin B3 deficiency. Indeed, mice fed a chow diet without vitamin B3, but with 0.23% Trp, were shown to maintain normal growth and a normal blood NAD(H) level.[12,13]

In mice or in vitro, NAD^+ deficiency has been successfully established through genetic manipulation or pharmaceutical intervention that aim to either disrupt NAD^+ synthesis or regeneration,[13–15] or to enhance NAD^+ consumption.[16,17] These strategies generally cause severe NAD^+ depletion and consequential physiological deterioration and provide important mechanistic insights, but are less human relevant since severe vitamin B3 deficiency is rare nowadays.[4]

Dr. W. Shi, Dr. M. A. Hegeman, A. Doncheva, I. van der Stelt, M. Bekkenkamp-Grovenstein, Dr. E. M. van Schothorst, Dr. V. C. J. de Boer, Prof. J. Keijer
Human and Animal Physiology
Wageningen University
PO Box 338, 6700 AH, Wageningen, The Netherlands
E-mail: jaap.keijer@wur.nl

Dr. M. A. Hegeman
Educational Consultancy & Professional Development
Faculty of Social and Behavioural Sciences, Utrecht University
3584 CS Utrecht, The Netherlands

Prof. C. Brenner
Department of Biochemistry
Carver College of Medicine, University of Iowa
Iowa City, IA 52242, USA

DOI: 10.1002/mnfr.201801100

The prevalence of mild vitamin B3 deficiency is, however, not well established, because clinical symptoms and physiological signs of vitamin B3 deficiency are relative unspecific.[8] Possibly, molecular responses to vitamin B3 withdrawal in mice could be used to provide more specific markers for mild vitamin B3 deficiency, a condition that is likely more common in human than severe deficiency.[4] Therefore, we aimed here to identify molecular responses to vitamin B3 withdrawal using global transcriptome analysis. We used NR as exclusive source of vitamin B3, as the optimal dietary level of this B3 vitamin has been established in mice and can be used as control.[18] We focused on epididymal white adipose tissue (eWAT), since we previously established eWAT as an organ that is sensitive to especially low levels of NR,[19] whereas effects of low NR were not seen in subcutaneous WAT, liver, or skeletal muscle (ref. 19 and unpublished data regarding the expression of energy metabolism genes for all three tissues and subcutaneous WAT adipocyte morphometry). Furthermore, diet-induced obesity induces an NAD^+ decline in eWAT.[20] In addition, in vitro studies have indicated that adipocyte differentiation is affected by vitamin B3 exposure.[21,22] We performed a dietary intervention in male C57BL/6JRccHsd mice using a diet without NR and with NR at the recommended vitamin B3 level. To identify effects, a large influx of NAD^+ from tryptophan had to be prevented and we therefore used a diet with a low, but adequate level of Trp (0.115%).

2. Experimental Section

2.1. Dosage Information

A semi-synthetic diet (Table S1, Supporting Information) was employed, containing 40% energy from fat, 41% energy from carbohydrates, and 19% energy from proteins, with a low but sufficient amount of tryptophan (calculated 0.115% L-tryptophan) and either 0 or 30 mg NR per kg diet as vitamin B3 source (referred to as No-NR and Ctrl-NR, respectively).

2.2. Animal Study

The animal experiment was ethically approved (DEC2016033b) and performed in full accordance with national and EU-regulations. This independent experiment was performed as part of a larger experiment to reduce the number of (control) animals. C57BL/6JRccHsd male mice (Envigo, Horst, the Netherlands) were individually housed (12 h light–dark cycle, 23 ± 1 °C, 55 ± 15% humidity), with ad libitum access to feed and water, unless indicated otherwise. Nine-week-old mice were accustomed to the Ctrl-NR diet for 2 weeks. Subsequently, mice were stratified based on their body weight into two experimental groups ($n = 12$ per group) and received the No-NR or Ctrl-NR diet for 18 weeks. Body parameters measurements, sample collection, and processing are in Methods, Supporting Information.

2.3. Metabolic Flexibility and Energy Expenditure

Indirect calorimetry was conducted in week 14 using a PhenoMaster System (TSE Systems, Bad Homburg, Germany), as described.[19] Respiratory exchange ratio (RER) and energy expenditure (EE) were obtained using TSE software. Metabolic flexibility was assessed based on the change of RER in response to a fasting-refeeding challenge as the incremental area under the RER curve (iAUC) between 16:00 h and 23:00 h, with the RER of each group at 16:00 h as baseline. The mean of EE of the fasted and the refeeding period were calculated. RER and EE were measured under the non-challenged conditions before the fasting-refeeding challenge.

2.4. Oral Glucose Tolerance Test

An oral glucose tolerance test (OGTT) was performed in week 17, as described[23] and detailed in Supporting Information Methods.

2.5. Circulating Parameters

Determination of circulating parameters and related calculations are in Methods, Supporting Information.

2.6. RNA Isolation

Total RNA was isolated from eWAT using Trizol combined with a RNeasy Mini kit (Qiagen, Venlo, the Netherlands), as described.[24] RNA isolation from liver and soleus was done as published.[19] RNA purity and yield were measured using Nanodrop (NanoDrop, Wilmington, USA) and RNA integrity was verified using TapeStation (Agilent, Santa Clara, CA, USA).

2.7. Genome Wide Gene Expression

Two-hundred nanograms RNA of each sample ($n = 12$ per group) was assayed using mouse whole genome 8 × 60 K microarrays (Agilent Technologies Inc., Santa Clara, CA, USA), as published.[25] Signals were extracted (Feature extraction 10.7.3.1., Agilent), quality controlled, and normalized as described.[25] All microarray data are MIAME compliant and were stored in GEO (GSE116483). 26 384 probes (44.0% of total) were considered expressed (average expression >2× background). 4795 probes were differentially expressed with a Benjamini–Hochberg false discovery rate adjusted Student's *t*-test *p* value of less than 0.5 (FDR < 0.5) and 368 probes were with FDR <0.2. Fold change is the ratio of mean expression of No-NR over Ctrl-NR. Probes with FDR <0.2 were used for the analysis of pathway maps and GO processes using MetaCore (Thomson Reuters, New York, USA). Genes enriched in the top 10 pathway maps were gathered and presented as a heatmap using GeneMaths XT (Applied Maths, Sint-Martens-Latem, Belgium). The top 30 down- and upregulated annotated genes with FDR <0.2 were annotated using public databases (MGI [www.informatics.jax.org], Nextprot [www.nexprot.org], and Pubmed [www.ncbi.nlm.nih.gov/pubmed]). From these, genes related to insulin sensitivity were selected and their net effect on insulin sensitivity was indicated, based on scientific literature (PubMed). Similarly,

from the FDR < 0.2 dataset, genes related to tetrahydrobiopterin (BH4) synthesis were selected, supplemented with relevant FDR < 0.5 genes and their net effect on BH4 synthesis was indicated. Mitochondrial gene expression was separately interrogated. Nuclear encoded mitochondrial genes extracted from the mouse MitoCarta2.0 database (https://www.broadinstitute.org/files/shared/metabolism/mitocarta/mouse.mitocarta.2.0.html), and the distribution of down- and upregulated probes was analyzed for FDR < 0.5 and for FDR < 0.2. Pathway analysis using MetaCore was performed based on the subset of "mitochondrial genes," in which we used FDR < 0.5 dataset to ensure a sufficient number of genes. The distribution of down- and upregulated probes for the top 10 pathway map was calculated.

2.8. qRT-PCR Validation

cDNA synthesis and regular qRT-PCR were performed as described.[19] Gene expression was presented as fold change of expression value normalized by reference genes with the mean value of Ctrl-NR at 1. Primer sequences are in Table S2, Supporting Information.

2.9. Immunohistochemistry

Fluorescence microscopy of glucose transporter type 4 (GLUT4/SLC2A4) was performed as described in Methods, Supporting Information. Adipocyte cell size as well as macrophages were measured as described,[19] with minor modifications and details as in Methods, Supporting Information.

2.10. Western Blot

Levels of mitochondrial oxidative phosphorylation (OXPHOS) complex proteins in eWAT were assessed by western blot using an OXPHOS antibody cocktail (Abcam, Cambridge, MA, USA) with total protein expression (REVERT Total Protein Stain, LI-COR, Lincoln, NE, USA) as control. Details are in Methods, Supporting Information.

2.11. Targeted NAD^+ Metabolites Analysis

NAD^+ metabolites were extracted from eWAT and liver and identified and quantified using LC-MS as described in Methods, Supporting Information.

2.12. Statistics

Data are expressed as mean ± SEM for $n = 10$ to 12 mice and $n = 6$ to 8 for immunohistochemistry. Statistical analysis was performed using GraphPad Prism v5.04 (San Diego, CA, USA). Data were verified for normality using the D'Agostino and Pearson omnibus normality test and log transformed if needed. Statistical differences were analyzed using two-way repeated measures ANOVA followed by Bonferroni post-hoc analysis or Students' *t*-test. p values <0.05 were considered statistically significant.

3. Results

3.1. Body Parameters and Metabolic Flexibility

Since vitamin B3 deficiency can affect health, we monitored progression of body weight and composition as well as metabolic parameters. We compared No-NR to Ctrl-NR, unless indicated otherwise. No significant differences were observed over the 18 week period in body weight, lean mass, fat mass, and feed intake (**Figure 1**A–D). In line with this, no significant differences were seen in RER or EE under non-challenged conditions (Figure S1, Supporting Information). Under fasting-refeeding challenge conditions, the Ctrl-NR animals tended to have a higher iAUC of RER ($p = 0.061$) (Figure 1E,G), suggesting that these animals were better able to switch from fatty acid oxidation (FAO) to carbohydrate oxidation (CHO) during the refeeding transition. No significant differences were seen in EE during the challenge test (Figure 1F,H). In the refed condition, glucose, triglycerides (TG), nonesterified fatty acids (NEFA), total cholesterol, HDL cholesterol, LDL cholesterol, leptin, and adiponectin, exhibited comparable circulating levels between groups (**Table 1**). The serum serotonin level, which is associated with tryptophan metabolism, was not changed in No-NR (Table 1).

3.2. Systemic Glucose Tolerance

An OGTT was performed to assess insulin-stimulated glucose clearance. The blood glucose levels and glucose iAUC did not differ between the No-NR and the Ctrl-NR animals during the OGTT (**Figure 2**A,B). The No-NR animals required higher levels of insulin, with a significantly elevated peak insulin level ($t = 15$ min) and a tendency toward a larger iAUC ($p = 0.083$; Figure 2C,D). These animals also exhibited significantly higher fasting circulating insulin levels (Figure 2E). HOMA-IR, an indicator of insulin resistance, was higher in No-NR (Figure 2F). These data implicate that mice on No-NR were less insulin sensitive.

3.3. eWAT Transcriptome Enrichment Analysis

WAT plays an important role in the regulation of metabolic flexibility and systemic insulin sensitivity.[26,27] Therefore, we focused on the molecular responses of WAT and performed a whole-genome transcriptome analysis of eWAT. The most affected pathways and GO-processes were bioinformatically established. In the top 10 pathways, developmental processes and white adipocyte differentiation stand out (**Figure 3**A). Eight of the top 10 GO processes were related to cellular localization (G5, G7, G8, G9) and intracellular transportation, including endosomal and cytoplasmic transport and regulation of Golgi (G1, G2, G3, G4) (Figure 3B). While the pathways and GO processes seemed to differ, the underlying genes were not.

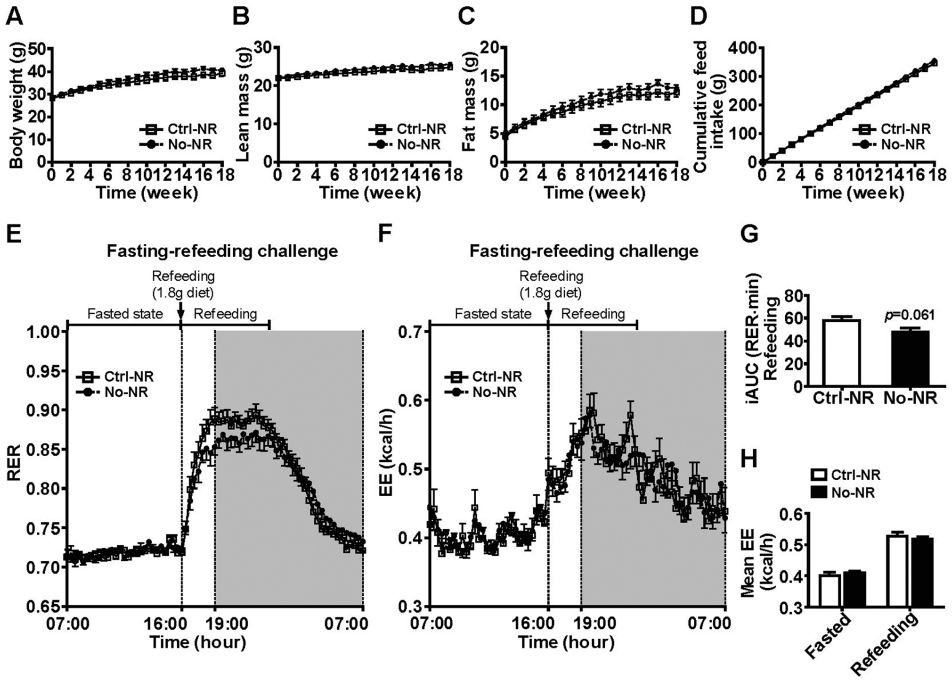

Figure 1. Whole body parameters and metabolic flexibility. A) Body weight, B) lean mass, C) fat mass, D) cumulative feed intake. E) Metabolic flexibility and F) EE in week 14. The challenge (1.8 g diet at 16.00 h) was given when the animals were fully fasted (on fatty acid oxidation) resulting in a switch to carbohydrate oxidation. The shaded area indicates the dark, active period. G) Metabolic flexibility was analyzed as incremental area under the RER curve (iAUC; baseline = mean of RER at 16:00 h) during the refeeding transition. H) Mean of EE for each period. Ctrl-NR: open square with solid line or white bar. No-NR: closed circle with black dashed line or black bar. Data as mean ± SEM, $n = 11$ to 12. Analysis with two-way ANOVA for (A)–(F), (H) and Students' *t*-test for (G).

Table 1. Circulating parameters.

Indicators[a]	Ctrl-NR		No-NR		*p* value[b]
	Mean	SEM	Mean	SEM	
Blood glucose [mmol L^{-1}]	5.9	0.2	5.7	0.2	0.290
TG [mg dL^{-1}]	131.6	7.0	127.3	7.9	0.692
NEFA [mmol L^{-1}]	1.1	0.1	1.1	0.1	0.906
Total cholesterol [mg dL^{-1}]	134.8	9.9	137.9	7.7	0.808
HDL cholesterol [mg dL^{-1}]	75.4	8.7	65.3	7.2	0.242
LDL cholesterol [mg dL^{-1}]	43.9	6.2	52.2	7.1	0.399
Leptin [mg mL^{-1}]	1.3	0.2	1.4	0.1	0.496
Adiponectin [mg mL^{-1}]	1.1	0.3	0.7	0.1	0.228
Serotonin [µg mL^{-1}]	12.0	1.7	12.0	1.1	0.972

[a] At necropsy (refed); [b] Students' *t*-test ($n = 10$ to 12).

The pathways were represented by a set of ten differentially expressed genes, with three genes appearing in all pathways: *Mapk1* (also known as *Erk2*), *Map2k1* (also known as *Mek1*), and *Map2k2* (also known as *Mek2*) (Figure 3C). *Mapk1* also appeared in all top 10 GO processes, while *Map2k1* and *Map2k2* were present in nine out of ten GO processes (Figure 3C). *Dnm2, Rdx*, and *Arghf1* were present in several pathway maps, while *Jak3, Ftna, Raptor*, and *Stim1* appeared in one pathway map. *Dmn2, Rdx, Jak3, Fnta*, and *Raptor* also appeared in the top 10 GO processes. Of these genes, *Mapk1, Map2k1*, and *Fnta* were upregulated, while the remainder were downregulated. Since pathway analysis suggested WAT differentiation, we examined eWAT morphological parameters (Figure S2, Supporting Information). In line with similar adiposity and eWAT weight (Figure S3A,B, Supporting Information), no significant differences were found in mean adipocyte size and its frequency distribution (Figure S3C–F, Supporting Information). In agreement with the data-analysis output that did not indicate inflammation, no differences in the number of crown-like structures (CLSs) or single macrophages were observed (Figure S3G,H, Supporting Information). The transcriptional expression of the genes related to adipogenesis and anti-oxidant response in eWAT were not significantly changed, in accordance with the lack of evident morphological changes (Table S5, Supporting Information).

3.4. eWAT Insulin Signaling

To obtain a more detailed insight in eWAT gene regulation in response to No-NR, the top 30 (fold change, FC) down- and up-regulated genes, FDR < 0.2 genes, were further studied (**Table 2**; Table S3, Supporting Information). Among the 60 genes, several are directly related to insulin signaling, including the lower expressed genes *Anp32a, Esr1, Ehd2, Tnk2* (also known as *Ack1*), *Pbrm1, Jak3*, and *Hk1* and the higher expressed genes *Map2k1, Meg3*, and *Mapk1* (**Figure 4**A and in bold in Table 2). Functional interpretation based on their direction of expression is consistently linked to a decreased activity of AKT,[28–37] implicating a

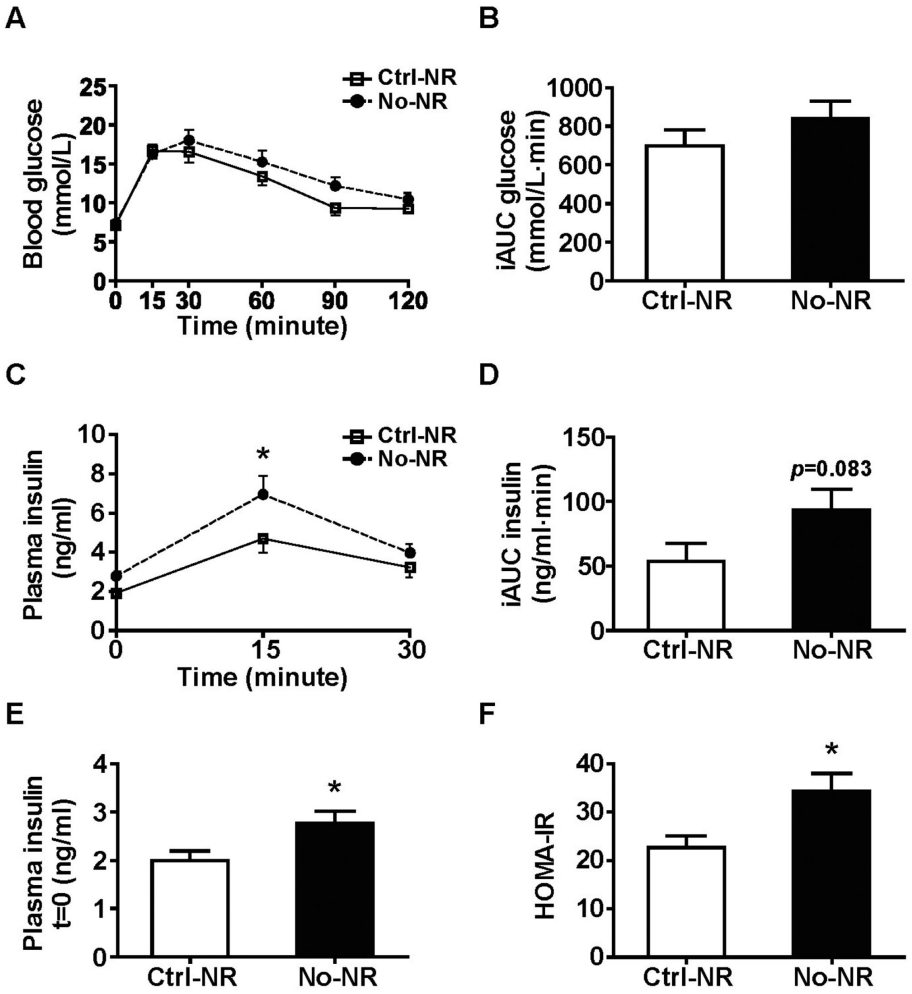

Figure 2. A) Oral glucose tolerance test. Blood glucose levels at the indicated time-points before and after an oral glucose administration in week 17. B) iAUC. Plasma insulin at indicated time-points during C) OGTT and D) plasma insulin iAUC (baseline is mean of $t = 0$ insulin in Ctrl-NR). E) Plasma insulin at $t = 0$. F) HOMA-IR. Ctrl-NR: open square with solid line or white bar. No-NR: closed circle with black dashed line or black bar. Data as mean ± SEM, $n = 11$ to 12. Analysis with two-way ANOVA for (A), (C) or Students' *t*-test for (B), (D)–(F). *$p < 0.05$.

downregulation of insulin signaling (Figure 4A). For technical validation, *Anp32a, Ehd2, Tnk2, Map2k1, and Mapk1* plus *Glut4* were selected and examined using qRT-PCR. All these genes, except *Ehd2*, were significantly or tended to be regulated, confirming the microarray data (Figure 4B). The gene expression of *Mapk1* and *Map2k1* was considerably higher in No-NR. The expression of *Tnk2* and *Anp32a* was more than twofold lower in No-NR. Expression of selected insulin signaling related genes that were affected in eWAT, was also examined in the liver and skeletal muscle, two other key organs controlling insulin sensitivity. However, no significant differences were observed in the gene expression of *Map2k1*, *Mapk1*, or *Glut2* in the liver nor of *Map2k1*, *Mapk1*, or *Glut4* in skeletal muscle (Figure S4, Supporting Information).

GLUT4 plays a key role in the downstream regulation of insulin signaling in WAT.[38] Since *Glut4* gene expression tended to be lower in No-NR ($p = 0.07$), we analyzed GLUT4 protein expression. Using fluorescence microscopy, we observed GLUT4 expression on the adipocytes. The intensity of the GLUT4 staining was markedly reduced in No-NR (Figure 4C), suggesting lower GLUT4 protein levels.

3.5. eWAT Mitochondria

Three mitochondrial genes *Mthfs (FC 1.7)*, *Mthfsl (FC 1.45)*, and *Qdpr* (FC 1.42) are among the most upregulated genes (Table 2). This was not due to a general upregulation of mitochondrial genes. Examining the 1661 mitochondrial probes in our dataset, derived from mouse MitoCarta 2.0, we found that 74.5% of the probes with FDR <0.5 were downregulated (5.0% for all expressed probes with FDR <0.5). This predominant downregulation was slightly more overt for FDR <0.2 (78,3%, while this was 4.9% for all expressed probes) (**Figure 5**A). The level of OXPHOS complex IV protein was decreased in No-NR, and the levels of proteins representing complex II, III, and V tended to be lower (Figure 5B), confirming the mitochondrial gene expression data.

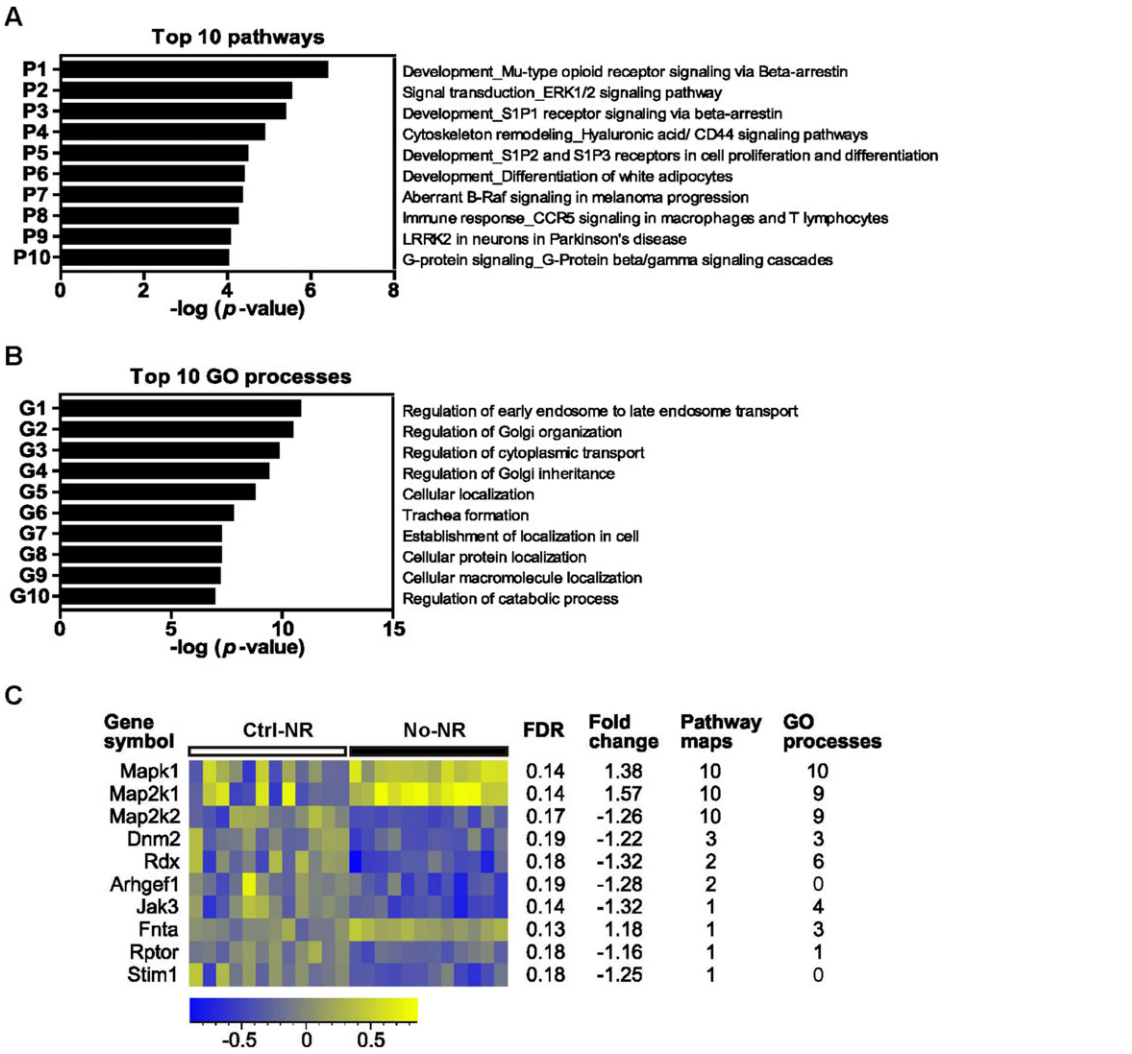

Figure 3. Transcriptome analysis of eWAT. A) The top 10 pathway maps. B) The top 10 GO processes. C) Significant genes in the top 10 pathway maps, their expression as heat map ($n = 12$), FDR, fold change (No-NR over Ctrl-NR), and number of times appearing in a top 10 pathway maps and GO processes. The expression is presented as absolute expression in a sample minus the mean of the respective gene.

An enrichment analysis of the FDR < 0.5 mitochondrial genes showed that the ubiquinone metabolism pathway was most affected (**Figure 6**A). Without exception, this pathway consisted of genes encoding for NADH:ubiquinone oxidoreductase subunits that compose mitochondrial OXPHOS Complex I, with the majority of these genes being downregulated (22/24, 91.7%; Figure 6B). Among the limited number of upregulated mitochondrial genes (FDR < 0.5) were four key fatty acid oxidation genes *Acsf2, Cpt1a, Etfa*, and *Slc25a20* (Figure 6C). This might indicate an increased fatty acid oxidation, supported by the lower RER of the No-NR group at all time-points over a 24 h period (Figure S1A, Supporting Information).

3.6. Implications in Tetrahydrobiopterin Synthesis in eWAT

The upregulation of the mitochondrial genes *Qdpr, Mthfs*, and *Mthfsl* was fully confirmed by qRT-PCR (**Figure 7**A). Since the function of QDPR is uniquely in salvaging of tetrahydrobiopteridin (BH4),[39] and *Mthfs* and *Mthfsl* are implicated in the de novo BH4 synthesis, the more extensive FDR < 0.5 gene list was examined for additional genes directly related to these processes. One gene associated with BH4 salvage, *Mthfd1*, and two genes related to the de novo BH4 synthesis, *Sumo2* and *Gchfr*, were identified (Figure 7B). The direction of expression of these six genes is consistent with the upregulation of BH4 synthesis[39–44] (Figure 7B).

3.7. Targeted NAD^+ Metabolites in eWAT and Liver

To assess NAD^+ status, levels of selected NAD^+ metabolites were quantified in the eWAT and the liver. Levels of NAD^+, $NADP^+$, ADPR, NMN, and Me4py (full names in Methods, Supporting Information) were not significantly altered in eWAT (**Figure 8**A–E). In the liver, the level of NMN, a marker of vitamin B3 exposure,

Table 2. Top 30 down- and upregulated unique genes (FDR < 0.2, No-NR over Ctrl-NR).

Gene symbol	Fold change	Gene symbol	Fold change
Anp32a	−1.95	***Mthfsl***	1.70
Isoc2a	−1.86	*Rnu3b1*	1.66
Fmr1nb	−1.76	*Gm10115*	1.64
DefB36	−1.72	***Map2k1***	1.57
Pakap	−1.59	*5330406M23Rik*	1.54
Ino80d	−1.52	***Tmem123***	1.52
Esr1	−1.47	***Dcc***	1.47
Cmtm4	−1.46	*Gmpr2*	1.46
Cd151	−1.45	***Mthfs***	1.45
Nr3c1	−1.45	***Qdpr***	1.42
Dtx1	−1.44	***Gcm1***	1.42
Rnd1	−1.44	*Rhox8*	1.42
Chtf8	−1.43	*LOC553096*	1.41
Akap11	−1.41	***Ermn***	1.41
4833439L19Rik	−1.38	***Sumo2***	1.40
Kdsr	−1.36	*Pnma2*	1.40
Ehd2	−1.35	*Gm33195*	1.40
Tnk2	−1.35	*Dynlt3*	1.40
Arl4d	−1.34	*Trpm1*	1.39
Abca2	−1.34	*B020031M17Rik*	1.39
Pbrm1	−1.34	*GaB3*	1.39
Rita1	−1.34	***Eif2a***	1.39
Arl6ip5	−1.33	***Meg3***	1.38
Chpf2	−1.33	*1700097N02Rik*	1.38
Rdx	−1.32	***Mapk1***	1.38
Mta1	−1.32	*4932431P20Rik*	1.38
Cxx1a	−1.32	*Slfn9*	1.38
Cldnd1	−1.32	*5033418A18Rik*	1.37
Jak3	−1.32	*D030002E05Rik*	1.37
Hk1	−1.32	*Zdhhc6*	1.36

Gene in bold are discussed. Gene annotation, systematic names, and gene function are in Table S3, Supporting Information.

was significantly lower in the No-NR group, whereas the levels of NAD^+, $NADP^+$, ADPR, NAAD, and Me4py remained unchanged (Figure 8F–H).

4. Discussion

Here, we observed a decreased insulin sensitivity in mice fed a vitamin B3 withdrawal diet. Since WAT was shown to be sensitive to vitamin B3 status,[19,45] we identified the molecular responses to vitamin B3 withdrawal in eWAT. The transcriptome data indicated a differential regulation of a set of genes involved in insulin signaling and lowering of markers of glucose utilization. Furthermore, biosynthesis of BH4, an essential cofactor for neurotransmitter synthesis, was found to be transcriptionally activated. A set of significant and strongly regulated genes related to these processes were technically validated and could serve as a WAT transcriptional signature marker for mild vitamin B3 deficiency. This signature is composed of downregulation of *Anp32a*,*Tnk2* and the upregulation of *Mapk1*, *Map2k1*, *Qdpr*, *Mthfs*, and *Mthfsl*.

To impose a vitamin B3 insufficiency stress, we provided male C57BL/6JRccHsd mice with a diet without vitamin B3 and a low, but sufficient, amount of Trp to limit the rate of de novo NAD^+ synthesis. The latter is essential to be able to observe effects of vitamin B3 withdrawal.[12,13] Due to cellular use of NAD^+, which has a high turnover rate,[3] and urinary secretion of NAD^+ breakdown metabolites, this diet should gradually lead to vitamin B3 insufficiency. After the 18 week intervention, no differences were seen between the No-NR group and the Ctrl-NR group in body weight, lean mass, fat mass, EE, WAT weight, adipocyte size, WAT inflammation, or a range of circulating markers, including circulating serotonin levels. This could suggest the absence of a functional effect of vitamin B3 withdrawal. However, both the lower level of NMN in the liver, as well as potential NAD^+ sparing molecular adaptations (see below), suggest functionality of the intervention. Maintenance of tissue NAD^+ levels may be supported by de novo NAD^+ synthesis from dietary Trp, which, at 0.115%, is just above minimal requirements.[10] Indeed, the level of NAAD, an intermediate of the de novo NAD^+ biosynthesis pathway, was not changed. By applying whole-genome transcriptome analysis, qRT-PCR and physiological analyses to eWAT, we were able to establish differential regulation of insulin signaling. A lowering in markers of glucose utilization and an increase in markers of fatty acid catabolism, implicate a shift from glucose to lipids for energy supply, which may be related to the reduced expression of the mitochondrial electron transport complexes. Finally, we observed transcriptional activation of the synthesis pathway of BH4, an essential cofactor for neurotransmitter synthesis.

The mild vitamin B3 deficiency resulted in a decreased insulin sensitivity. The underlying mechanisms were molecularly traceable in WAT. The top 10 GO processes center on the regulation of intracellular transport and localization (Figure 3B), which play an important role in insulin signal transduction and especially in downstream glucose transporter trafficking.[46] The downregulation of most of the genes involved in these GO processes potentially implicate a downregulation of insulin signaling in the No-NR group (Figure 3C). This is supported by decrease in the activation state of AKT, a key node in growth factor/insulin mediated glucose uptake[47] (Figure 4A). GLUT4, the major glucose transporter in adipocytes, was lower expressed in No-NR (Figure 4C). GLUT4 is responsible for insulin-stimulated glucose uptake, and lower expression of GLUT4 is associated with local as well as systemic insulin sensitivity.[48] The transcriptional activation of MEK/ERK may be implicated in a downregulation of insulin signaling as well. MEK/ERK activation was shown to decrease insulin-stimulated glucose uptake, concomitant with the downregulation of *Glut4* and the reduced glucose oxidation in adipocytes.[49,50]

The upregulation of *Map2k1* (*Mek1*) and *Mapk1* (*Erk2*) indicate MEK/ERK activation. In agreement, *Eif2a* and *Gcm1*, targets of activated MEK/ERK,[35,51] were also upregulated (Table 2). *Map2k2* (*Mek2*) was transcriptionally decreased, which might be due to the feedback regulation of an activated MEK/ERK pathway.[52] We also technically validated the twofold downregulation of *Anp32a (Pp32)*, which is the most responsive gene in the dataset. Its downregulation is in line with MEK/ERK activation,

A

Assignment of genes from Table 2 to net effect on insulin sensitivity

Gene symbol	Fold change	Function	Net effect on insulin sensitivity	Reference
Anp32a	-1.95	Positively regulates AKT phosphorylation	Down	[28]
Esr1	-1.47	Positively regulates AKT phosphorylation and IRS1 activity	Down	[29]
Ehd2	-1.35	Plays a role in insulin-induced GLUT4 recruitment	Down	[30]
Tnk2	-1.35	Activates AKT phosphorylation at tyrosine 176 site	Down	[31]
Pbrm1	-1.34	Activates AKT phosphorylation and glucose uptake	Down	[32]
Jak3	-1.32	Activates AKT phosphorylation	Down	[33]
Hk1	-1.32	Promotes glycolysis and associated with AKT activation	Down	[34]
Mapk1	1.38	Inhibits AKT phosphorylation	Down	[35]
Meg3	1.38	Inhibits phosphorylation of PI3K and AKT	Down	[36]
Map2k1	1.57	Inhibits AKT phosphorylation	Down	[37]

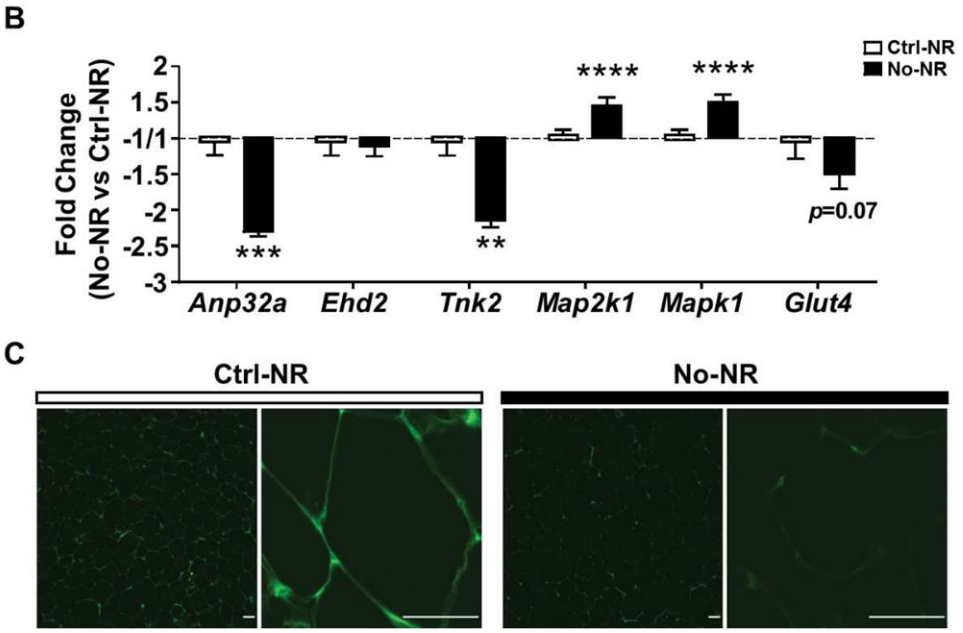

Figure 4. Insulin sensitivity. A) The net effect on insulin sensitivity of eWAT genes related to insulin signaling (from top regulated genes, Table 2). B) Validation of selected insulin signaling related genes using qRT-PCR. Gene expression as No-NR over Ctrl-NR ($n = 11$ to 12). Ctrl-NR: white bar, No-NR: black bar. Data as mean ± SEM. Analysis with Students' *t*-test. $^{**}p < 0.01$, $^{***}p < 0.005$, $^{****}p < 0.001$. C) Representative pictures for expression of GLUT4: Ctrl-NR left (10× magnification), right (63×); No-NR left (10× magnification), right (63×). $n = 6$. Scale bar 50 µm.

since silencing of *Anp32a* has been shown to induce MEK/ERK activation.[53] Of note, all of the top 10 pathway maps and 9 of the top 10 GO processes contain *Mapk1* and *Map2k1*, validating these genes as the core of the transcriptional signature of vitamin B3 deficiency in eWAT.

Concomitant with decreased levels of GLUT4, the gene expression of hexokinase 1 (HK1), that controls the initial rate-limiting step of glycolysis, is downregulated, indicating that glucose utilization is inhibited in WAT of the No-NR animals. Meanwhile, key mitochondrial FAO genes were upregulated (Figure 6C), contrasting with the downregulation of glycolysis and overall downregulation of mitochondrial genes (Figure 5A). This suggests a shift from CHO to FAO in the No-NR animals, supported by a reduced ability to switch from FAO to CHO (from a fasted RER of 0.7 to a refed RER approaching 1.0; Figure 1E), and the 24 h RER being lower at all time-points in No-NR (Figure S1A, Supporting Information), confirming previously published data.[19] This may be explained by the lower requirement for NAD^+ of FAO, compared to aerobic CHO, to produce the same amount of ATP. Supporting this explanation, the RER was distinctly decreased upon the transition to a high fat diet in WAT-specific *Nampt* knockout mice displaying WAT NAD^+ deficiency,[14] suggesting a clear preference of FAO compared to control. In WAT of No-NR animals, we also observed a preferred downregulation of the mitochondrial Complex I genes (Figure 6B) and reduced expression of OXPHOS Complex IV (Figure 5B), coinciding with the putatively inhibited glucose utilization. OXPHOS Complex I accepts electrons from NADH, possibly implicating that the downregulation serves to liberate NAD^+ for other cellular functions. Indeed, NAD^+ level was not changed by vitamin B3 withdrawal (Figure 8A) and NAD^+ biosynthesis or other consumer genes were absent from FDR < 0.2 gene set (data not shown). The lower levels of GLUT4, of *Hk1* expression and of mitochondrial Complex I gene expression, and the increased FAO genes molecularly support a bioenergetic shift to liberate NAD^+ for other processes, providing a possible

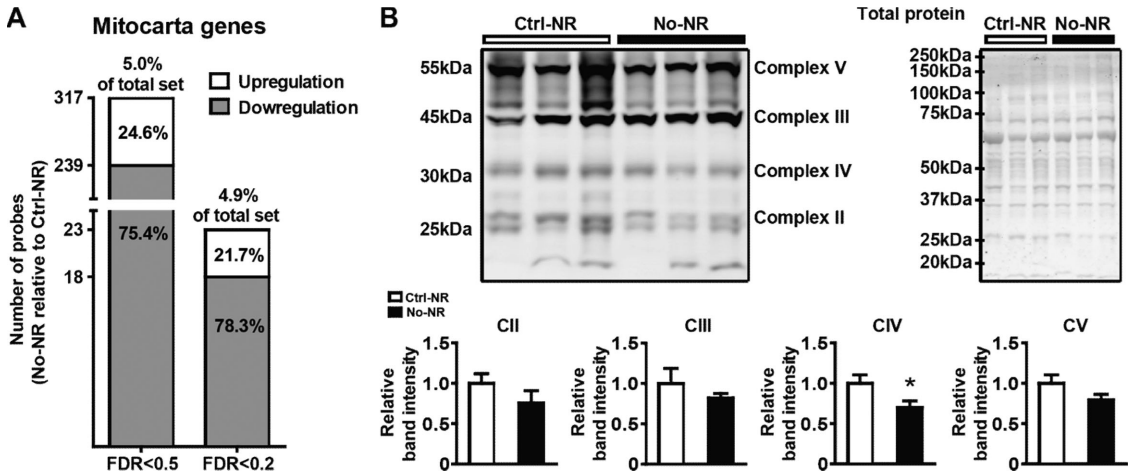

Figure 5. Mitochondrial gene analysis and OXPHOS protein expression. A) Distribution of down- and upregulated (No-NR over Ctrl-NR) eWAT mitochondrial genes ($n = 12$) according to Mouse MitoCarta 2.0, up/down distribution in FDR < 0.5 set and FDR < 0.2 set. Upregulation; white bar, Downregulation: grey bar. B) OXPHOS Complex II-V proteins, total protein loading control and quantified Complex II-V intensity. Ctrl-NR: white bar, No-NR: black bar. Analysis with Students' *t*-test analysis (mean ± SEM; $n = 7$).

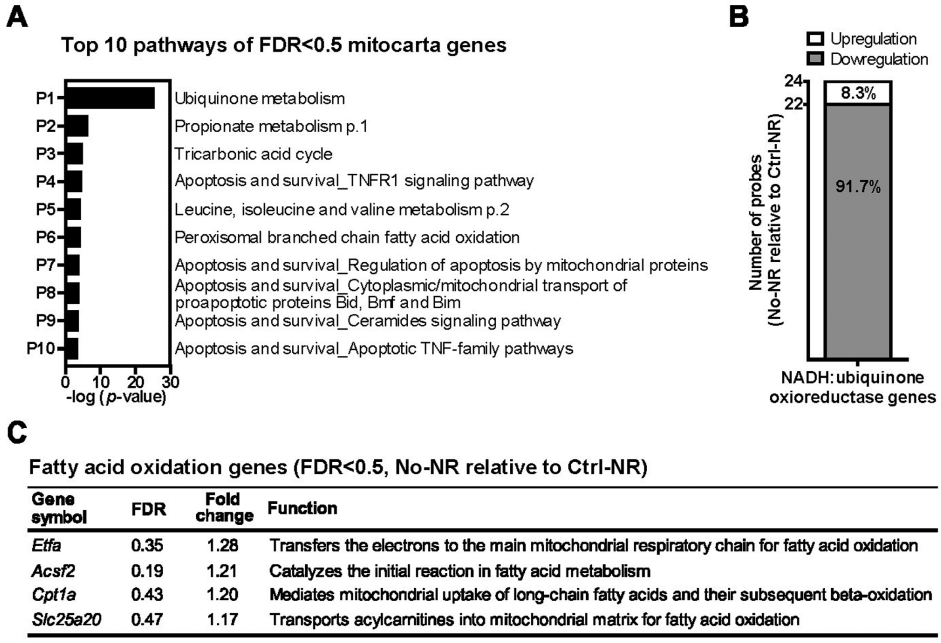

C

Fatty acid oxidation genes (FDR<0.5, No-NR relative to Ctrl-NR)

Gene symbol	FDR	Fold change	Function
Etfa	0.35	1.28	Transfers the electrons to the main mitochondrial respiratory chain for fatty acid oxidation
Acsf2	0.19	1.21	Catalyzes the initial reaction in fatty acid metabolism
Cpt1a	0.43	1.20	Mediates mitochondrial uptake of long-chain fatty acids and their subsequent beta-oxidation
Slc25a20	0.47	1.17	Transports acylcarnitines into mitochondrial matrix for fatty acid oxidation

Figure 6. Enrichment analysis of mitochondrial genes. A) Pathway maps analysis of FDR < 0.5 mitochondrial genes. B) Distribution of up-/downregulated genes in the top 10 pathway ubiquinone metabolism. C) Fatty acid oxidation genes. $n = 12$. Upregulation: white bar, Downregulation: grey bar. Gene names and systemic names are in Table S4, Supporting Information.

mechanistic explanation for the reduced metabolic flexibility of the mice on the vitamin B3 withdrawal diet.

An intriguing finding of this study was the upregulation of *Qdpr*, *Mthfs*, and *Mthfsl* (Figure 7A), which sharply contrasts with the downregulation that was observed for the majority of mitochondrial genes (Figure 5A). *Mthfs* and *Qdpr* have an established role in pteridine metabolism. *Mthfs* encodes 5-formyltetrahydrofolate cyclo-ligase (MTHFS) that irreversibly catalyses the conversion of 5-formyltetrahydrofolate, also known as folinic acid, to 5,10-methenyltetrahydrofolate.[40] *Qdpr* encodes quinoid dihydropteridine reductase (QDPR) with a unique function in the salvage synthesis of BH4 from dihydrobiopterin (BH2).[39] The concurrent elevation of *Mthfs* and *Qdpr*, and possibly also structurally related *Mthfsl*, may indicate an enhanced interconnection between folate metabolism and BH4 salvage synthesis. In the brain, MTHFS, QDPR, and MTHFD1 have been proposed to cooperate in support of the BH4 pool as a favorable pathway to bypass the "methyl trap."[41] Of note, this pathway requires NADH as an essential cofactor, resulting in a release of NAD^+. Downregulated *Gchfr*[42,43] and upregulated *Mthfs*[44] and *Sumo2*[40] support an increased de novo BH4 biosynthesis (Figure 7B). It has been shown that the stimulation

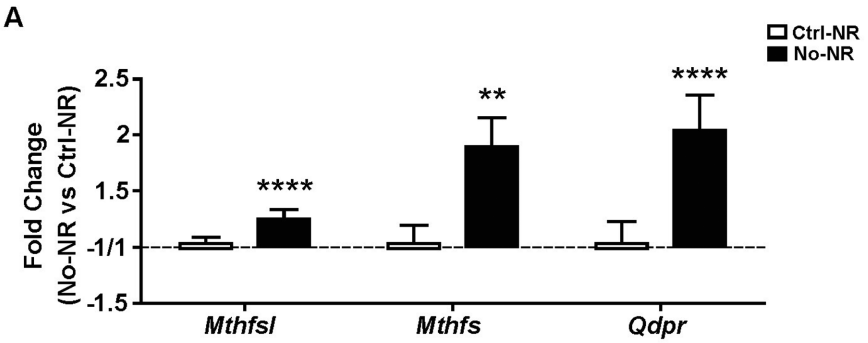

B

Assignment of genes from FDR<0.5 to net effect on BH4 synthesis (No-NR relative to Ctrl-NR)

Gene symbol	Fold change	FDR	Function	Net effect on BH4 synthesis	Reference
Mthfsl	1.70	0.14	Similarity with MTHFS function is indicated	Up	n. a.
Mthfs	1.45	0.17	Involves folinic acid-induced BH4 salvage synthesis via 5-MTHF; or enhances yield of GTP, a *de novo* precursor of BH4, via promoting *de novo* purine synthesis	Up	[41,44]
Qdpr	1.42	0.14	Mediates BH4 salvage synthesis	Up	[39,41]
Sumo2	1.40	0.13	MTHFS-induced *de novo* purine synthesis requires SUMO	Up	[40]
Mthfd1	1.16	0.34	Together with MTHFS, involving folinic acid-induced BH4 salvage synthesis	Up	[41]
Gchfr	-1.38	0.40	Negatively regulates *de novo* BH4 synthesis from GTP by inhibiting GCH1 activity	Up	[42,43]

Figure 7. Tetrahydropteridin (BH4) biosynthesis. A) Validation of expression of selected genes in eWAT using qRT-PCR. B) Relevant genes were assigned according to their net effect on BH4 synthesis. Gene expression as fold change of No-NR over Ctrl-NR. Ctrl-NR: white bar. No-NR: black bar. Data as mean ± SEM. Analysis with Students' *t*-test. $^{**}p < 0.01$, $^{****}p < 0.001$. $n = 11$ to 12.

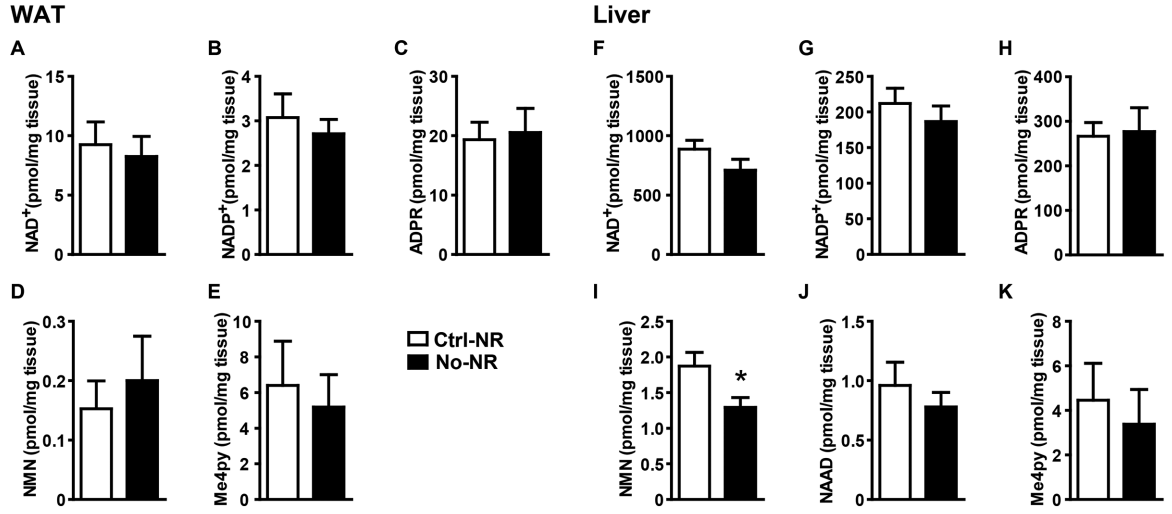

Figure 8. NAD metabolome analysis. A–E) The levels of NAD^+, $NADP^+$, ADPR, NMN, and Me4py in the eWAT. F–K) The levels of NAD^+, $NADP^+$, ADPR, NMN, NAAD, and Me4py in the liver. Ctrl-NR: white bar. No-NR: black bar. Data as mean ± SEM. Analysis with Students' *t*-test. $^{*}p < 0.05$. $n = 3$ to 7.

of this pathway by folinic acid or folic acid is effective as treatment of genetic defects of QDPR, that display abnormal low BH4 levels.[39,41] The observed gene expression changes are in line with a published metabolomics analysis of in vitro NAMPT silencing that showed an enhanced folate metabolism and de novo purine synthesis,[54] that may potentiate BH4 biosynthesis.

Neural signals have an important role in the regulation of the WAT metabolic function.[55,56] In the current study, the No-NR mice displayed an upregulation of *Dcc*, *Gcm1*, *Ermn*, *Pnma2*, and *Tmem123* (Table 2), genes with a proven role in neuronal cell survival and maturation,[57–61] possibly indicating an effect on WAT innervation. BH4 serves as an essential cofactor for tryptophan hydroxylase (TPH), phenylalanine hydroxylase, tyrosine hydroxylase as well as nitric oxide synthases. BH4 thus plays a vital role in the generation of neurotransmitters, such as serotonin, dopamine, and nitric oxide. It is tempting to speculate that the upregulation of BH4 synthesis serves to support the neuronal regulation of WAT metabolic function. To fully establish why increased BH4 synthesis occurs following vitamin B3 withdrawal and how this affects WAT metabolism awaits more detailed dedicated experimentation.

In conclusion, the current study showed an impaired insulin sensitivity in mice with mild vitamin B3 deficiency. Molecularly examined in WAT, the underlying metabolism is putatively associated with MEK/ERK activation and liberation of NAD^+ from oxidative glucose metabolism to other NAD^+ dependent cellular functions. Our data also implicate a possible increase in BH4 synthesis, which is an essential cofactor in neurotransmitter biosynthesis. We propose the expression of seven technically validated FDR < 0.2 genes related to these processes, the downregulation of *Anp32a, Tnk2* and the upregulation of *Mapk1, Map2k1, Qdpr, Mthfs*, and *Mthfsl*, as a WAT transcriptional signature marker for mild vitamin B3 deficiency.

Supporting Information

Supporting Information is available from the Wiley Online Library or from the author.

Acknowledgements

The authors thank ChromaDex for the generous and kind supply of nicotinamide riboside. The authors thank their colleagues at Human and Animal Physiology and the animal facility for their help. The authors thank Ruth Van Heerbeek for practical contributions. Financial support by the Chinese Scholarship Council (grant #201303250054) is gratefully acknowledged. W.S., V.C.J.B., M.A.H., and J.K. were responsible for the study concept and design; W.S. conducted the animal experiment; W.S., A.D., I.S., and M.B.-G. performed biochemical, molecular, and histological analyses; W.S. and E.M.S. performed bioinformatics; C.B. performed targeted NAD^+ metabolomics. W.S. performed statistical analysis and wrote the draft manuscript. W.S., V.C.J.B., and J.K. interpreted the data and finalized the manuscript.

Conflict of Interest

Charles Brenner is inventor of intellectual property related to uses of nicotinamide riboside, which have been licensed by ChromaDex, Inc. He owns ChromaDex stock and serves as their chief scientific adviser. He is on the scientific advisory board of Cytokinetics, Inc. All other authors declare no conflict of interest.

Keywords

biomarkers, deficiency, MEK/ERK, tetrahydropteridine, vitamin B3

Received: October 11, 2018
Revised: March 11, 2019
Published online: April 26, 2019

[1] L. Rajman, K. Chwalek, D. A. Sinclair, *Cell Metab*. **2018**, *27*, 529.
[2] W. Ying, *Antioxid. Redox Signal*. **2008**, *10*, 179.
[3] L. Liu, X. Su, W. J. Quinn, 3rd, S. Hui, K. Krukenberg, D. W. Frederick, P. Redpath, L. Zhan, K. Chellappa, E. White, M. Migaud, T. J. Mitchison, J. A. Baur, J. D. Rabinowitz, *Cell Metab*. **2018**, *27*, 1067.
[4] P. Wan, S. Moat, A. Anstey, *Br. J. Dermatol.* **2011**, *164*, 1188.
[5] J. M. Rawling, T. M. Jackson, E. R. Driscoll, J. B. Kirkland, *J. Nutr.* **1994**, *124*, 1597.
[6] J. M. Rawling, T. M. Jackson, B. D. Roebuck, G. G. Poirier, J. B. Kirkland, *Nutr. Cancer* **1995**, *24*, 111.
[7] M. K. Horwitt, A. E. Harper, L. M. Henderson, *Am. J. Clin. Nutr.* **1981**, *34*, 423.
[8] J. B. Kirkland, in *Handbook of Vitamins* (Eds: J. Zempleni, J. W. Suttie, J. F. Gregory III, P. J. Stover), CRC Press, Boca Raton **2013**, Ch. 5.
[9] D. A. Bender, *Nutritional Biochemistry of the Vitamins*, Cambridge University Press, London **2003**.
[10] National Research Council, *Nutrient Requirements of Laboratory Animals*, 4th Rev. ed., National Academies Press, Washington DC **1995**.
[11] J. G. Fox, S. Barthold, M. Davisson, C. E. Newcomer, F. W. Quimby, A. Smith, *The Mouse in Biomedical Research: Diseases*, Academic Press, Salt Lake City, UT **2006**.
[12] M. Terakata, T. Fukuwatari, E. Kadota, M. Sano, M. Kanai, T. Nakamura, H. Funakoshi, K. Shibata, *J. Nutr.* **2013**, *143*, 1046.
[13] M. Terakata, T. Fukuwatari, M. Sano, N. Nakao, R. Sasaki, S.-I. Fukuoka, K. Shibata, *J. Nutr.* **2012**, *142*, 2148.
[14] K. N. Nielsen, J. Peics, T. Ma, I. Karavaeva, M. Dall, S. Chubanava, A. L. Basse, O. Dmytriyeva, J. T. Treebak, Z. Gerhart-Hines, *Mol. Metab.* **2018**, *11*, 178.
[15] D. W. Frederick, E. Loro, L. Liu, A. Davila, Jr., K. Chellappa, I. M. Silverman, W. J. Quinn, S. J. Gosai, E. D. Tichy, J. G. Davis, F. Mourkioti, B. D. Gregory, R. W. Dellinger, P. Redpath, M. E. Migaud, E. Nakamaru-Ogiso, J. D. Rabinowitz, T. S. Khurana, J. A. Baur, *Cell Metab*. **2016**, *24*, 269.
[16] J. Camacho-Pereira, M. G. Tarrago, C. C. S. Chini, V. Nin, C. Escande, G. M. Warner, A. S. Puranik, R. A. Schoon, J. M. Reid, A. Galina, E. N. Chini, *Cell Metab*. **2016**, *23*, 1127.
[17] H. Yamamoto, Y. Uchigata, H. Okamoto, *Nature* **1981**, *294*, 284.
[18] P. Bieganowski, C. Brenner, *Cell* **2004**, *117*, 495.
[19] W. Shi, M. A. Hegeman, D. A. M. van Dartel, J. Tang, M. Suarez, H. Swarts, B. van der Hee, L. Arola, J. Keijer, *Mol. Nutr. Food Res.* **2017**, *61*, 1600878.
[20] S. Liu, T.-H. Kim, D. A. Franklin, Y. Zhang, *Cell Rep*. **2017**, *18*, 1005.
[21] J. E. Lewis, Y. Shimizu, N. Shimizu, *FEBS Lett.* **1982**, *146*, 37.
[22] K. W. Ryu, T. Nandu, J. Kim, S. Challa, R. J. DeBerardinis, W. L. Kraus, *Science* **2018**, *360*, eaan5780.
[23] L. P. Duivenvoorde, E. M. van Schothorst, H. M. Swarts, O. Kuda, E. Steenbergh, S. Termeulen, J. Kopecky, J. Keijer, *PLoS One* **2015**, *10*, e0128515.
[24] F. P. Hoevenaars, M. Bekkenkamp-Grovenstein, R. J. Janssen, S. G. Heil, A. Bunschoten, E. F. Hoek-van den Hil, S. Snaas-Alders, K. Teerds, E. M. van Schothorst, J. Keijer, *Mol. Nutr. Food Res.* **2014**, *58*, 799.

[25] E. M. van Schothorst, V. Pagmantidis, V. C. J. de Boer, J. Hesketh, J. Keijer, *Anal. Biochem.* **2007**, *363*, 315.
[26] L. Storlien, N. Oakes, D. Kelley, *Proc. Nutr. Soc.* **2004**, *63*, 363.
[27] L. M. Sparks, B. Ukropcova, J. Smith, M. Pasarica, D. Hymel, H. Xie, G. A. Bray, J. M. Miles, S. R. Smith, *Diabetes Res. Clin. Pract.* **2009**, *83*, 32.
[28] W. Yan, Z. Bai, J. Wang, X. Li, B. Chi, X. Chen, *Oncol. Rep.* **2017**, *38*, 1605.
[29] V. Ribas, M. A. Nguyen, D. C. Henstridge, A.-K. Nguyen, S. W. Beaven, M. J. Watt, A. L. Hevener, *Am. J. Physiol. Endocrinol. Metabol.* **2009**, *298*, E304.
[30] S. Y. Park, B. G. Ha, G. H. Choi, J. Ryu, B. Kim, C. Y. Jung, W. Lee, *Biochemistry* **2004**, *43*, 7552.
[31] K. Mahajan, D. Coppola, S. Challa, B. Fang, Y. A. Chen, W. Zhu, A. S. Lopez, J. Koomen, R. W. Engelman, C. Rivera, R. S. Muraoka-Cook, J. Q. Cheng, E. Schonbrunn, S. M. Sebti, H. S. Earp, N. P. Mahajan, *PLoS One* **2010**, *5*, e9646.
[32] B. Chowdhury, E. G. Porter, J. C. Stewart, C. R. Ferreira, M. J. Schipma, E. C. Dykhuizen, *PLoS One* **2016**, *11*, e0153718.
[33] H. Wang, J. Brown, S. Gao, S. Liang, R. Jotwani, H. Zhou, J. Suttles, D. A. Scott, R. J. Lamont, *J. Immunol.* **2013**, *191*, 1164.
[34] K. Gottlob, N. Majewski, S. Kennedy, E. Kandel, R. B. Robey, N. Hay, *Genes Dev*. **2001**, *15*, 1406.
[35] S. Shin, G. R. Buel, L. Wolgamott, D. R. Plas, J. M. Asara, J. Blenis, S. O. Yoon, *Mol. Cell* **2015**, *59*, 382.
[36] X. Zhu, Y. B. Wu, J. Zhou, D. M. Kang, *Biochem. Biophys. Res. Commun.* **2016**, *469*, 319.
[37] M. Fujishiro, Y. Gotoh, H. Katagiri, H. Sakoda, T. Ogihara, M. Anai, Y. Onishi, H. Ono, M. Abe, N. Shojima, Y. Fukushima, M. Kikuchi, Y. Oka, T. Asano, *Mol. Endocrinol.* **2003**, *17*, 487.
[38] P. E. Scherer, *Diabetes* **2006**, *55*, 1537.
[39] A. Ponzone, M. Spada, S. Ferraris, I. Dianzani, L. de Sanctis, *Med. Res. Rev.* **2004**, *24*, 127.
[40] M. S. Field, D. D. Anderson, P. J. Stover, *Front Genet*. **2011**, *2*, 36.
[41] S. Kaufman, *Neurochem. Res.* **1991**, *16*, 1031.
[42] M. A. Richardson, L. L. Read, C. L. T. Clelland, M. A. Reilly, H. M. Chao, R. W. Guynn, R. F. Suckow, J. D. Clelland, *Neuropsychobiology* **2005**, *52*, 190.
[43] L. Xie, J. A. Smith, S. S. Gross, *J. Biol. Chem.* **1998**, *273*, 21091.
[44] M. S. Field, D. M. Szebenyi, P. J. Stover, *J. Biol. Chem.* **2006**, *281*, 4215.
[45] J. Yoshino, K. F. Mills, M. J. Yoon, S. Imai, *Cell Metab*. **2011**, *14*, 528.
[46] L. J. Foster, D. Li, V. K. Randhawa, A. Klip, *J. Biol. Chem.* **2001**, *276*, 44212.
[47] C. M. Taniguchi, B. Emanuelli, C. R. Kahn, *Nat. Rev. Mol. Cell Biol.* **2006**, *7*, 85.
[48] C. J. Carlson, S. Koterski, R. J. Sciotti, G. B. Poccard, C. M. Rondinone, *Diabetes* **2003**, *52*, 634.
[49] J. M. Brown, M. S. Boysen, S. Chung, O. Fabiyi, R. F. Morrison, S. Mandrup, M. K. McIntosh, *J. Biol. Chem.* **2004**, *279*, 26735.
[50] L. Liu, M. Zhou, H. Lang, Y. Zhou, M. Mi, *J. Cell. Mol. Med.* **2018**, *22*, 1247.
[51] V. Nadeau, J. Charron, *Development* **2014**, *141*, 2825.
[52] S.-K. Hong, P.-K. Wu, M. Karkhanis, J.-I. Park, *Cell. Signal.* **2015**, *27*, 1939.
[53] C. Fukukawa, N. Tanuma, T. Okada, K. Kikuchi, H. Shima, *Cancer Lett.* **2005**, *226*, 155.
[54] R. K. Singh, L. van Haandel, D. P. Heruth, S. Q. Ye, J. S. Leeder, M. L. Becker, R. S. Funk, *J. Pharmacol. Exp. Ther.* **2018**, *365*, 96.
[55] H. Jiang, X. Ding, Y. Cao, H. Wang, W. Zeng, *Cell Metab*. **2017**, *26*, 686.
[56] T. J. Bartness, Y. B. Shrestha, C. H. Vaughan, G. J. Schwartz, C. K. Song, *Mol. Cell. Endocrinol.* **2010**, *318*, 34.
[57] M. Shi, M. H. Zheng, Z. R. Liu, Z. L. Hu, Y. Huang, J. Y. Chen, G. Zhao, H. Han, Y. Q. Ding, *Dev. Biol.* **2010**, *348*, 87.
[58] T. Takekoshi, Y. Tada, T. Watanabe, M. Sugaya, T. Hoashi, M. Komine, T. Kawashima, T. Shimizu, C. S. Hau, A. Asahina, T. Yokomizo, S. Sato, K. Tamaki, *J. Biol. Chem.* **2010**, *285*, 31876.
[59] Y. Altshuller, N. G. Copeland, D. J. Gilbert, N. A. Jenkins, M. A. Frohman, *FEBS Lett*. **1996**, *393*, 201.
[60] D. Brockschnieder, H. Sabanay, D. Riethmacher, E. Peles, *J. Neurosci.* **2006**, *26*, 757.
[61] O. Stich, S. Jarius, B. Kleer, C. Rasiah, R. Voltz, S. Rauer, *J. Neuroimmunol.* **2007**, *183*, 220.